Results in Physics 6 (2016) 1161–1167

Contents lists available at ScienceDirect

Results in Physics

journal homepage: www.journals.elsevier.com/results-in-physics

Influence of heterogeneous-homogeneous reactions in thermally stratified stagnation point flow of an Oldroyd-B fluid

T. Hayat [a,b], Zakir Hussain [a,*], A. Alsaedi [b]

[a] Department of Mathematics, Quaid-I-Azam University 45320, Islamabad 44000, Pakistan
[b] Nonlinear Analysis and Applied Mathematics (NAAM) Research Group, Department of Mathematics, Faculty of Science, King Abdulaziz University, P. O. Box 80257, Jeddah 21589, Saudi Arabia

ARTICLE INFO

Article history:
Received 20 October 2016
Received in revised form 4 November 2016
Accepted 17 November 2016
Available online 27 November 2016

Keywords:
Homogeneous-heterogeneous reactions
Thermally stratified fluid
Mixed convection
Stagnation point
Oldroyd-B fluid

ABSTRACT

This communication explores the effects of homogeneous-heterogeneous reactions in thermally stratified mixed convection flow of an Oldroyd-B fluid. Flow situation is addressed when the diffusion coefficients of the reactant and auto catalyst are equal. The stagnation point flow towards a stretching surface is discussed. Mathematical equations are developed for velocity, temperature and concentration functions through boundary layer theory. Resulting differential systems are computed for the convergent series solutions. Influences of various pertinent variables on the velocity, temperature and concentration are discussed. Comparison of present study is shown with the previous results. The outcomes are found in very good agreement.

Introduction

Analysis for the flows of non-Newtonian fluids is a topic of present research. Recent workers have shown keen interest in this area of research due to their numerous applications in industry, physiology, pharmaceuticals etc. The non-Newtonian fluids subject to their diverse characteristics cannot be described by one constitutive relationship. This fact of non-Newtonian materials is quite distinct than the viscous fluids. Accordingly many models of non-Newtonian fluids have been suggested in literature. Amongst these models the differential type fluids have been studied widely. It is due to the fact that the stress components in such fluids can be easily expressible in terms of velocity components. However in case of rate type fluids namely Maxwell, Oldroyd-B models etc this argument does not hold in general. Hence the flows involving rate type fluids is limited especially for two-dimensional situation. Note that the relaxation time effects can be described by Maxwell fluid model whereas the Oldroyd-B fluid explains both the relaxation and retardation times [1–8]. On the other hand the boundary layer stagnation point flow has been acknowledged by the investigators due to its occurrence in many areas of engineering and aerospace technology. Stagnation point flow examples are submarines over the tips of oil ships, rockets and aircraft. Hiemenz [9] explored firstly the boundary layer stagnation point flow of viscous fluid. Turkyilmazoglu et al. [10] examined exact analytical solutions for the stagnation point flow of Jeffrey fluid towards a stretching surface with heat transfer. Mukhopadhyay [11] investigated effects of partial slip on chemically reactive solute in stagnation point flow past stretching permeable sheet. Hayat et al. [12] presented thermally stratified stagnation point flow of Casson fluid subject to slip conditions. Furthermore the mixed convection flow has vital role in cooling of electronic devices, nuclear reactors cooled during emergency shutdown, solar energy systems, automobile demister, flows in the atmosphere and ocean etc. The study of convective heat transfer in a stratified fluid is considerable in practical applications such as exclusion of heat to the environment (rivers, lakes, sea), thermal energy storage systems (solar ponds) and thermal sources (condensers of power plants). Rashidi et al. [13] discussed mixed convective heat transfer for magnetohydrodynamic viscoelastic fluid flow by porous wedge with thermal radiation. Shehzad et al. [14] discussed three-dimensional mixed convection flow of Jeffrey fluid with thermophoresis and thermal radiation. Zheng et al. [15] addressed mixed convection heat transfer in flow of power law fluids by moving conveyor along an inclined plate. Few more studies [16–20] about mixed convection can be consulted.

There is no doubt that many natural processes involve both homogeneous and heterogeneous reactions. Except in the existence of a catalyst many reactions have the capacity to progress

* Corresponding author.
E-mail address: zakir.qamar@yahoo.com (Z. Hussain).

http://dx.doi.org/10.1016/j.rinp.2016.11.034
2211-3797/

gradually or not on the spot. There is composite relation between the homogeneous and heterogeneous reactions. Homogeneous/heterogeneous reaction are used in combustion, catalysis and biochemical mechanisms etc. Merkin et al. [21] studied a simple isothermal model for homogeneous-heterogeneous reactions in boundary-layer flow. Bhattacharyya et al. [22] analyzed boundary layer flow in porous medium through diffusion of chemically reactive species by porous plate. Hayat et al. [23] reported influence of homogeneous/heterogeneous reactions and melting heat transfer in viscoelastic fluid flow. Characteristics of Newtonian heating and homogeneous-heterogeneous reactions in the stagnation point flow with carbon nanotubes is explored by Hayat et al. [24]. Hayat et al. [25] addressed effects of homogeneous-heterogeneous reaction in flow of nanofluid through variable sheet thickness. Imtiaz et al. [26] reported MHD flow of Jeffrey fluid by a curve stretching sheet with convective condition and homogeneous-heterogeneous reactions. Hayat et al. [27] investigated influence of homogeneous-heterogeneous reactions in stagnation point flow with Cattaneo-Christov heat flux. Farooq et al. [28] reported impact of homogeneous-heterogeneous reaction in flow of Jeffrey fluid. Hayat et al. [29] studied homogeneous-heterogeneous reactions impact in flow with Joule heating and viscous dissipation. Having such in mind, the purpose here is to explore the analysis of Ref. [30] for homogeneous-heterogeneous reactions. The convergent of series solutions are obtained by Homotopy Analysis Method (HAM) [31–44]. Nusselt number is analyzed through graphical illustrations. A comparison between the homotopic and numerical solutions is also examined.

Formulation

We are interested to explore thermally stratified mixed convective flow [3–8] in stagnation region of an incompressible Oldroyd-B fluid. Fluid flow is considered under the influence of heterogeneous-homogeneous reactions. Due to small velocity the viscous dissipation is ignored. Thermal radiation is not account. The heat generated is accounted negligible for the irreversible chemical reaction. Cubic auto catalysis homogeneous reaction can be defined by

$$\mathbf{A} + 2\mathbf{B} \rightarrow 3\mathbf{B}, \quad rate = k_1 a_1 b_1^2, \tag{1}$$

and the isothermal reaction (first order) at the surface is given by

$$\mathbf{A} \rightarrow \mathbf{B}, \quad rate = k_s a. \tag{2}$$

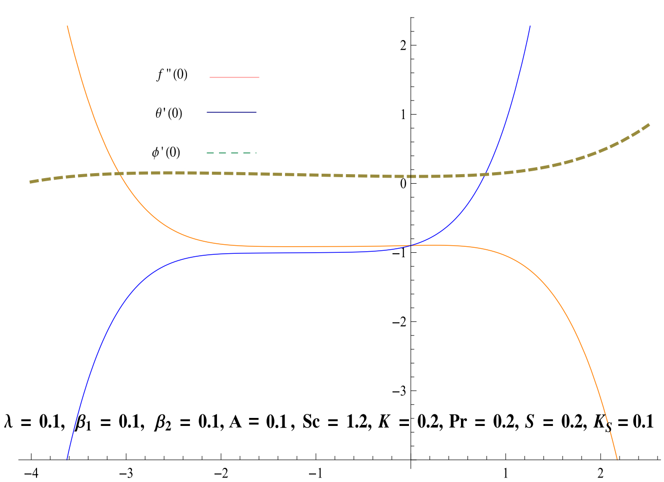

Fig. 1. The $\hbar$-curves.

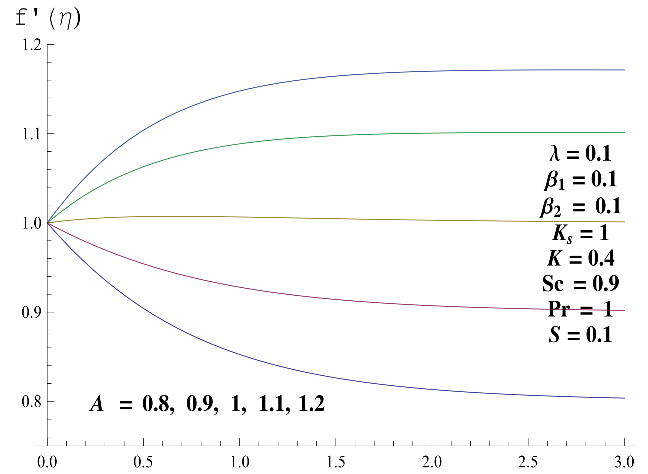

Fig. 2. Plots of A for f'.

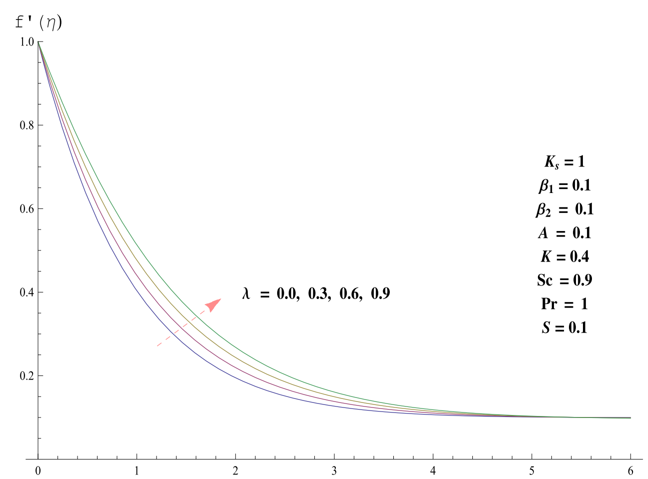

Fig. 3. Plots of λ for f'.

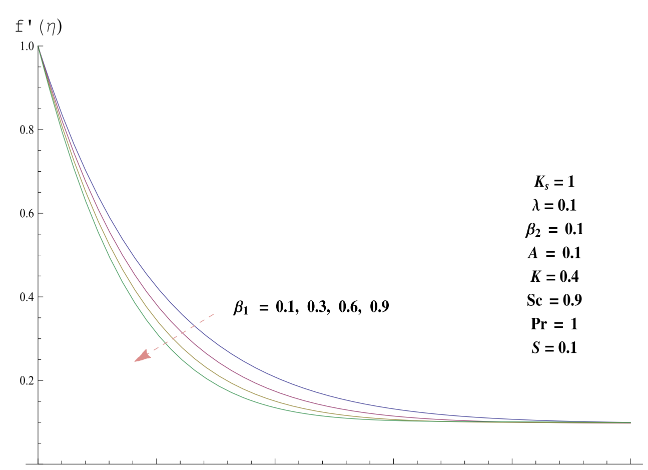

Fig. 4. Plots of β_1 for f'.

In above a_1 and b_1 the concentrations of chemical species of **A** and **B** correspondingly and k_1 and k_s the rate constants. Flow is persuaded by two equal amount of forces in opposite direction due to stretching of sheet keeping origin fixed and $u_w(x)$ and $u_e(x)$ the stretching velocity and the free stream velocity respectively. The relevant equations can be put into the forms:

$$\frac{\partial u}{\partial x}+\frac{\partial v}{\partial y}=0, \tag{3}$$

$$u\frac{\partial u}{\partial x}+v\frac{\partial u}{\partial y}+\lambda_1\left(u^2\frac{\partial^2 u}{\partial x^2}+v^2\frac{\partial^2 u}{\partial y^2}+2uv\frac{\partial^2 u}{\partial x\partial y}\right)=u_e\frac{du_e}{dx}$$
$$+\lambda_1 u_e^2\frac{d^2u_e}{dx^2}+\nu\frac{\partial^2 u}{\partial y^2}+\nu\lambda_2\left\{u\frac{\partial^3 u}{\partial x\partial y^2}+v\frac{\partial^3 u}{\partial y^3}-\frac{\partial u}{\partial x}\frac{\partial^2 u}{\partial y^2}-\frac{\partial u}{\partial y}\frac{\partial^2 u}{\partial y^2}\right\}$$
$$+g\beta_T(T-T_\infty), \tag{4}$$

$$\rho C_p\left(u\frac{\partial T}{\partial x}+v\frac{\partial T}{\partial y}\right)=K_1\frac{\partial^2 T}{\partial y^2}, \tag{5}$$

$$\begin{aligned}&u\tfrac{\partial a_1}{\partial x}+v\tfrac{\partial a_1}{\partial y}=D_A\tfrac{\partial^2 a_1}{\partial y^2}-k_1a_1b_1^2,\\&u\tfrac{\partial b_1}{\partial x}+v\tfrac{\partial b_1}{\partial y}=D_B\tfrac{\partial^2 b_1}{\partial y^2}+k_1a_1b_1^2.\end{aligned} \tag{6}$$

The corresponding boundary conditions are presented as follows:

$$\begin{aligned}&u=u_w(x)=cx,\ v=0,\ T=T_w=T_0+bx,\\&D_A\tfrac{\partial a_1}{\partial y}=k_sa_1,\ D_B\tfrac{\partial b_1}{\partial y}=-k_sa_1\quad \text{at}\quad y=0,\\&u=u_e(x)=ax,\ T\to T_\infty=T_0+dx,\\&a_1\to a_0,\ b_1\to 0\quad \text{as}\quad y\to\infty\end{aligned} \tag{7}$$

where u, v the components of velocity in x- and y-directions respectively, $\lambda_{1,}$ the relaxation time and λ_2 the retardation times respectively, g the gravitational acceleration, β_T the thermal expansion coefficient, υ the kinematic viscosity, ρ the density, C_p the specific heat, K_1 the thermal conductivity, a, b, c, d and a_0 the constants, D_A and D_B the respective diffusion coefficients, T_w and T_∞ the temperatures of the plate and ambient fluid respectively. Note that the Oldroyd-B fluid case is reduced to Maxwell and viscous material when $\lambda_1=0$ and $\lambda_i(i=1,2)=0$ respectively. Considering the transformations

$$u=cxf'(\eta),\ v=-\sqrt{c\nu}f(\eta),\ \eta=\sqrt{\frac{c}{\nu}}y,\ \theta=\frac{T-T_\infty}{T_w-T_0},$$
$$\phi(\eta)=\frac{a_1}{a_0},\ h(\eta)=\frac{b_1}{a_0}, \tag{8}$$

an incompressibility condition (3) is satisfied automatically while other equations become

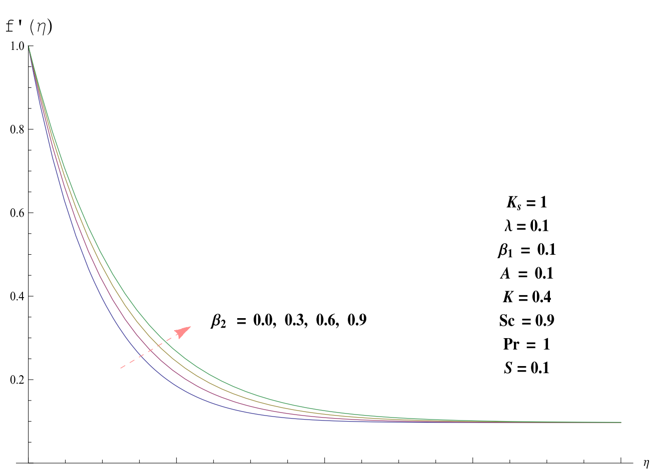

Fig. 5. Plots of β_2 for f'.

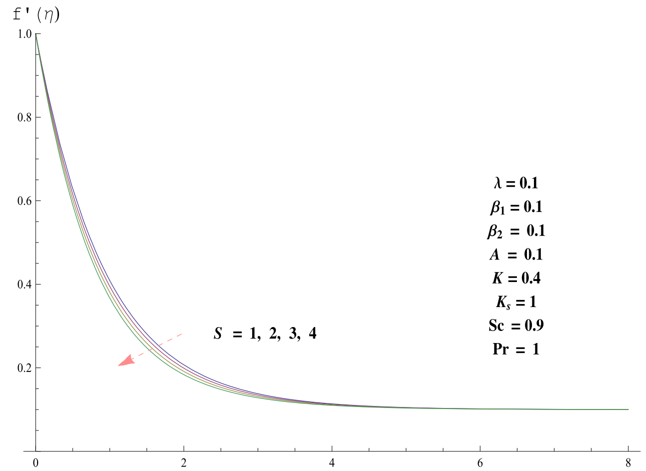

Fig. 6. Plots of S for f'.

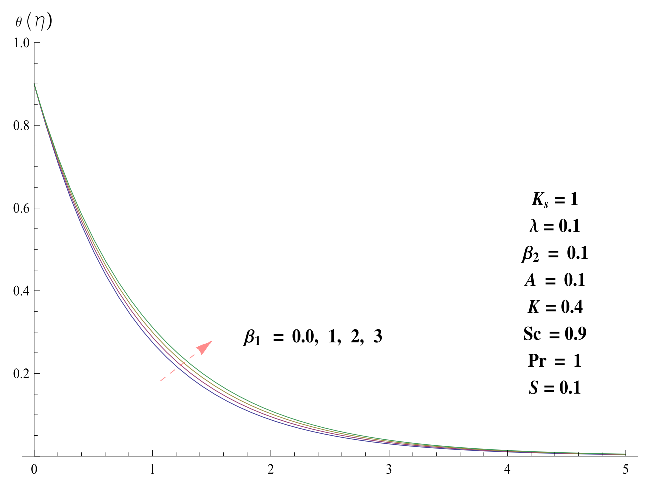

Fig. 7. Plots of β_1 for θ.

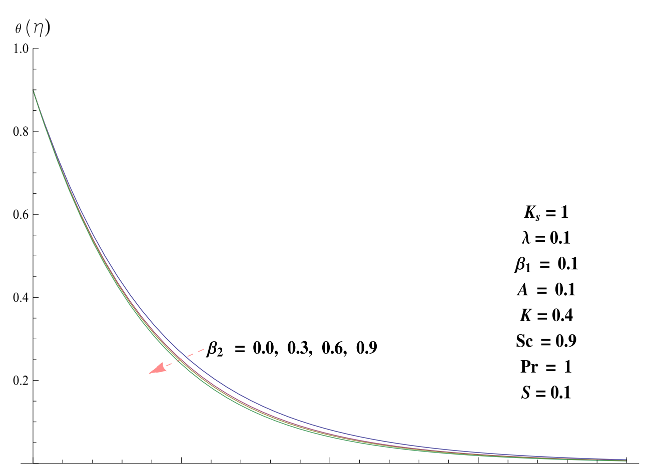

Fig. 8. Plots of β_2 for θ.

$$f'''-f'^2+ff''+A^2+\beta_1(2ff'f''-f^2f''')+\beta_2(f''^2-ff^{iv})+\lambda\theta=0, \tag{9}$$

$$\theta''-Pr(f'\theta-f\theta'+Sf')=0, \tag{10}$$

$$\phi''+Scf\phi'-ScK\phi(1-\phi)^2=0, \tag{11}$$

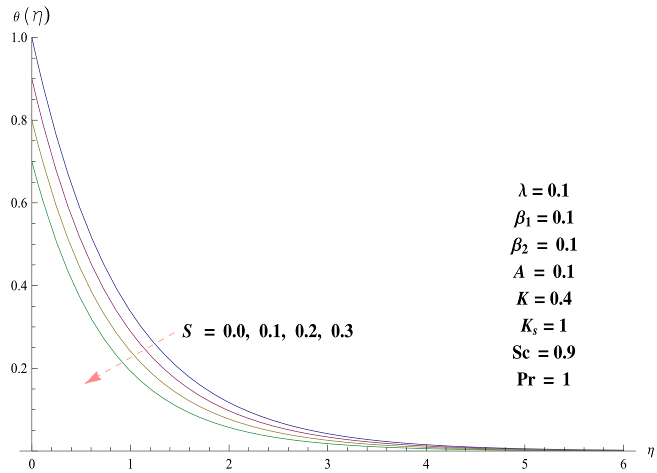

Fig. 9. Plots of S for θ.

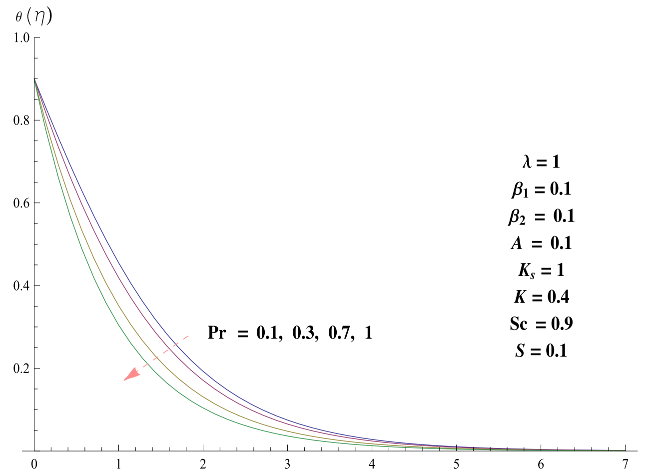

Fig. 12. Plots of Pr for θ.

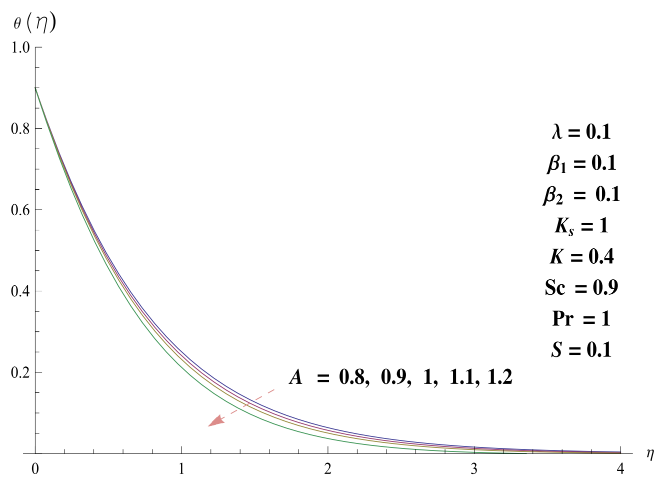

Fig. 10. Plots of A for θ.

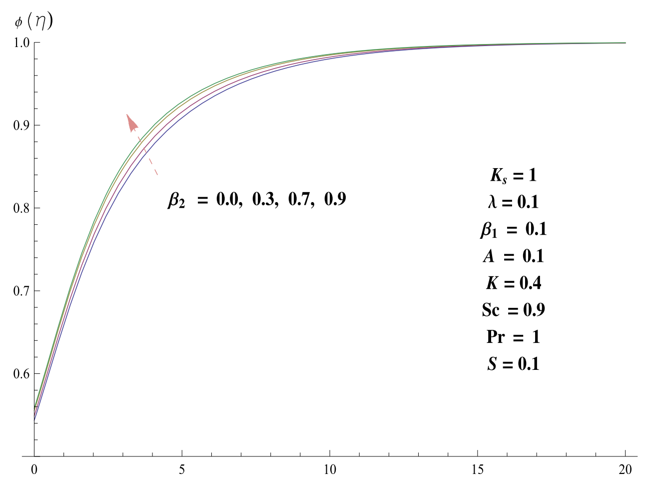

Fig. 13. Plots of β_2 for ϕ.

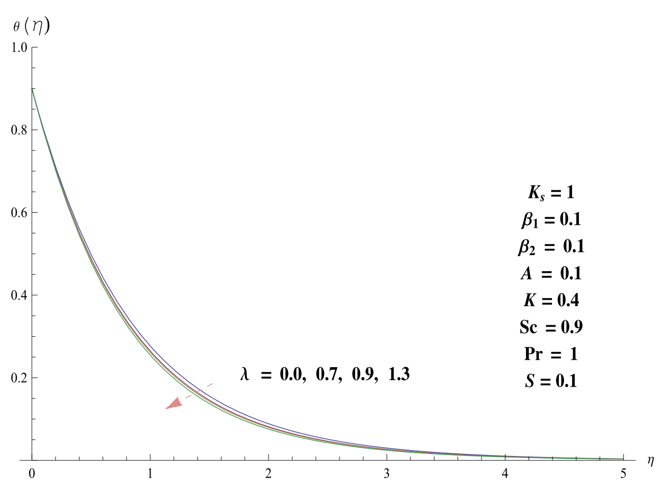

Fig. 11. Plots of λ for θ.

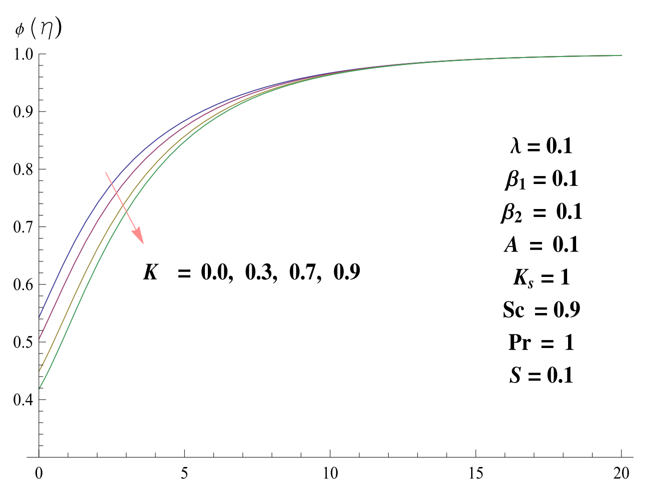

Fig. 14. Plots of K for ϕ.

$$
\begin{aligned}
&f(\eta)=0,\ f'(\eta)=1,\ \theta(\eta)=1-S,\ \phi'(\eta)=K_s\,\phi(\eta)\ \text{ at } \eta=0,\\
&f'(\eta)=A,\ \theta(\eta)=0,\ \phi(\eta)=1\quad \text{as}\quad \eta\to\infty,
\end{aligned}
\tag{12}
$$

where A represents the ratio of rates of free stream to stretching velocities, $\beta_1,$ β_2 the Deborah numbers in terms of relaxation and retardation times respectively, λ the mixed convection parameter, Pr the Prandtl number, S the thermally stratified parameter, Gr_x the Grashof number, Re_x the local Reynolds number, K measures the strength of homogeneous reaction, Sc the Schmidt number and K_s the strength of heterogeneous reaction. These involved parameters are given below:

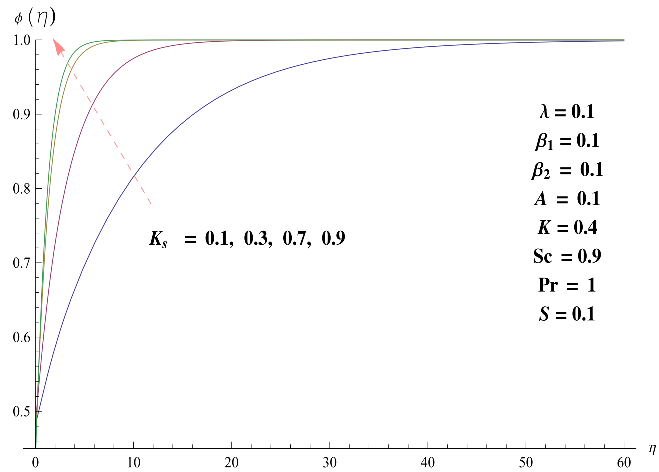

Fig. 15. Plots of Ks for ϕ.

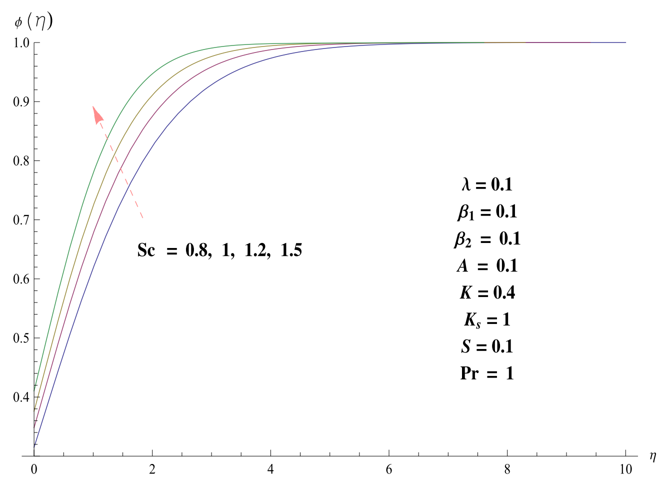

Fig. 16. Plots of Sc for ϕ.

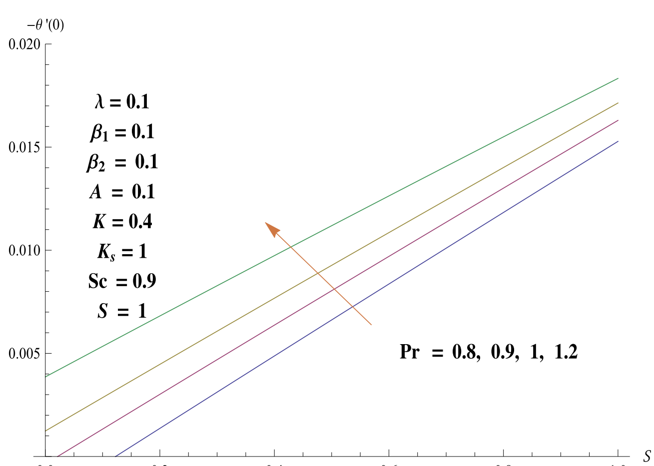

Fig. 17. Plots of Pr and S for $-\theta'(0)$.

$$\lambda = \frac{Gr_x}{\mathrm{Re}_x^2},\ Gr_x = \frac{g\beta_T(T_w - T_0)x^3}{\nu^2},\ \mathrm{Re}_x = \frac{u_e(x)x}{\nu},\ A = \frac{a}{c},\ \mathrm{Pr} = \frac{\mu C_p}{K_1},$$
$$S = \frac{d}{b},\ \beta_1 = \lambda_1 c,\ \beta_2 = \lambda_2 c,\ K = \frac{k_1 a_0^2}{c},\ Sc = \frac{\nu}{D_A},\ K_s = \frac{k_s}{D_A}\sqrt{\frac{\nu}{c}}. \tag{13}$$

Dimensionless local Nusselt number is defined in the following fashion:

$$Nu_x \mathrm{Re}^{-\frac{1}{2}} = -\theta'(0). \tag{14}$$

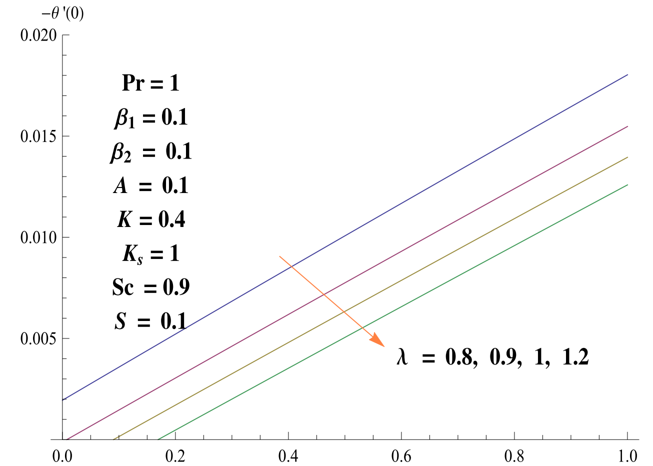

Fig. 18. Plots of λ *and* S for $-\theta'(0)$.

Series solutions

The initial guesses $(f_0,\ \theta_0, \phi_0)$ and auxiliary linear operators $(\mathcal{L}_f, \mathcal{L}_\theta, \mathcal{L}_\phi)$ for the problems under consideration are

$$f_0(\eta) = A\eta + (1 - A)(1 - \exp(-\eta)),\ \ \theta_0(\eta) = \exp(-\eta)(1 - S),$$
$$\phi_0(\eta) = \left(1 - \frac{1}{2}\exp(-k_s\eta)\right), \tag{15}$$

$$\mathcal{L}_f = \frac{d^3 f}{d\eta^3} - \frac{df}{d\eta},\ \mathcal{L}_\theta = \frac{d^2\theta}{d\eta^2} - \theta,\ \mathcal{L}_\phi = \frac{d^2\phi}{d\eta^2} - \phi, \tag{16}$$

$$\begin{aligned}&\mathcal{L}_f[C_1 + C_2\exp(\eta) + C_3\exp(-\eta)] = 0,\\ &\mathcal{L}_\theta[C_4\exp(\eta) + C_5\exp(-\eta)] = 0,\\ &\mathcal{L}_\phi[C_6\exp(\eta) + C_7\exp(-\eta)] = 0,\end{aligned} \tag{17}$$

in which C_i $(i = 1 - 7)$ indicate the arbitrary constants. The general solutions of resulting systems in terms of special solutions are

$$f_m(\eta) = f_m^*(\eta) + C_1 + C_2\exp(\eta) + C_3\exp(-\eta), \tag{18}$$

$$\theta_m(\eta) = \theta_m^*(\eta) + C_4\exp(\eta) + C_5\exp(-\eta), \tag{19}$$

$$\phi_m(\eta) = \phi_m^*(\eta) + C_6\exp(\eta) + C_7\exp(-\eta), \tag{20}$$

in which $f_m^*(\eta), \theta_m^*(\eta)$ and $\phi_m^*(\eta)$ are the special solutions. The values of constants through the boundary condition (12)

$$\begin{aligned}&C_2 = C_4 = C_6 = 0,\ C_3 = \left.\frac{\partial f_m^*(\eta)}{\partial\eta}\right|_{\eta=0},\ C_1 = -C_3 - f_m^*(0),\\ &C_5 = -(\theta_m'^*(0)),\ C_7 = \frac{1}{1+K_s}(\phi_m'^*(0) - K_s(\phi_m^*(0))).\end{aligned} \tag{21}$$

Convergence of the derived solutions

Note that to determine convergence region via homotopy analysis method is very important. The $\hbar$-curves in Fig. 1 shows the convergence region. The acceptable ranges of the auxiliary variables $\hbar_f$, $\hbar_\theta$ and $\hbar_\phi$ are $-1.5 \leqslant \hbar_f \leqslant -0.1$, $-2.5 \leqslant \hbar_\theta \leqslant -0.1$ and $-1.9 \leqslant \hbar_\phi \leqslant -0.8$.

Discussion

Interest in present section is to examine the effects of different parameters on the velocity, temperature and concentration profiles. Fig. 2 shows the variation of ratio parameter A for the velocity. There is enhancement of the velocity and boundary layer thickness *i.e* $(A < 1)$. The velocity function enhances while boundary layer thickness reduces *i.e* ($A > 1$). Variations of mixed convection variable for the velocity distribution is plotted in Fig. 3. It is seen that the velocity as well as layer thickness increase for larger mixed convection variable. We have now discussed the change in velocity and thermal boundary layer thickness with the variation in parameters. Fig. 4 is sketched for the plots of Deborah number β_1 in terms of relaxation time on the velocity. It is noted that velocity distribution decreases for larger values of Deborah number β_1. The plots of Deborah number β_2 for velocity is sketched in Fig. 5. It is seen that the velocity and boundary layer thickness enhance for larger values of Deborah number β_2. Fig. 6 is sketched for the influence of stratified parameter S on velocity field. It is observed that velocity field and boundary layer thickness are decreasing function of stratified parameter S. Influence of Deborah number β_1 on the temperature is displayed in Fig. 7. Temperature enhances with an increase in β_1. The thermal boundary layer also increases. Plots of Deborah number β_2 for temperature profile is shown in Fig. 8. Temperature and thermal boundary layer thickness decrease by increasing β_2. For example, in Fig. 8 it is seen that temperature curves approach free stream condition at larger values of η for larger Deborah number β_2. Thus thermal boundary layer thickness is a decreasing functions of β_2. Variations of stratified parameter on temperature profile is shown in Fig. 9. Here both temperature and thermal boundary thickness decrease with the increase in stratified parameter. Influence of ratio parameter A on the temperature is displayed in Fig. 10. Higher values of ratio variable correspond to reduction of temperature gradient. Influence of mixed convection parameter λ on temperature gradient is plotted in Fig. 11. Thermal boundary layer thickness declines with an increment in mixed convection parameter λ. Influence of Prandtl number is displayed in Fig. 12. Temperature profile decreases with an increase in Pr. Fig. 13 is plotted for influence of Deborah number β_2 on concentration distribution. Larger values of Deborah number β_2 correspond to enhancement of concentration profile. The plots of K for concentration distribution is shown in Fig. 14. The concentration decreases while solutal layer thickness enhances for larger values of homogeneous variable. Plots for the behavior of heterogeneous variable Ks for concentration distribution is sketched in Fig. 15. It is noticed that concentration decreases near the surface and it shows enhancement away from the surface for larger values of Ks. Impact of Schmidt number on concentration distribution is shown via Fig. 16. The concentration shows increasing behavior for larger Schmidt number. In fact Schmidt number is defined as the ratio of momentum to mass diffusivity. Hence larger values of Schmidt number correspond to very small mass diffusivity as a result the concentration distribution reduces. Fig. 17 is for the effects of Prandtl number Pr and stratification parameter S. Large values of Prandtl number lead to enhance the Nusselt number. Similar behavior is observed for stratification parameter S. Fig. 18 is sketched for the influence of mixed convection parameter and stratification parameter S. Here Nusselt number decreases via mixed convection parameter. However large stratification parameter shows an enhancement in Nusselt number. The convergence of

Table 1
Convergence of series solutions for different order of approximations when $\beta_1 = 0.1$, $\beta_2 = 0.1$, $A = 0.1$, $\lambda = 0.1$, $\Pr = 1$, $S = 0.1$, $K = 0.4$, $Ks = 1$, $Sc = 0.9$ and $\hbar = -0.9$.

Order of approximations	$-f''(0)$	$-\theta'(0)$	$\phi'(0)$
2	0.89416	0.95400	0.40572
6	0.90486	0.97746	0.35907
12	0.90876	0.98626	0.34164
18	0.91064	0.98902	0.33705
24	0.91064	0.99032	0.33520
30	0.91064	0.99032	0.33520

Table 2
Comparison of $f''(0)$ for different values of β_1, β_2 and A when $\lambda = 0$ through the Refs. [1,45,46,30]. Here PR denotes the present results.

	Newtonian fluid ($\beta_1 = 0, \beta_2 = 0$)					Maxwell fluid ($\beta_1 = 0.2, \beta_2 = 0$)			Oldroyd-B fluid ($\beta_1 = 0.2, \beta_2 = 0.2$)		
A	Ref. [45]	Ref. [46]	Ref. [1]	Ref. [30]	PR	Ref. [1]	Ref. [30]	PR	Ref. [1]	Ref. [30]	PR
0.01		−0.9980	−0.9981	−0.9963	−0.9933	−1.0499	−1.0428	−1.0400	−0.9583	−0.9560	−0.9510
0.02		−0.9958	−0.9958	−0.9930	−0.9915	−1.0476	−1.0394	−1.0354	−0.9567	−0.9531	−0.9500
0.05		−0.9876	−0.9876	−0.9830	−0.9811	−1.0393	−1.0296	−1.0255	−0.9490	−0.9460	−0.9430
0.10	−0.9694	−0.9694	−0.9694	−0.9603	−0.9590	−1.0207	−1.0124	−1.0100	−0.9330	−0.9296	−0.9266
0.20	−0.9181	−0.9181	−0.9181	−0.9080	−0.9060	−0.9681	−0.9675	−0.9576	−0.8890	−0.8875	−0.8833
0.50	−0.6673	−0.6673	−0.6673	−0.6605	−0.6585	−0.7078	−0.7082	−0.6980	−0.6549	−0.6578	−0.6578
1.00		0.0000	0.0000	0.0000	0.0000	0.0000	0.0000	0.0000	0.0000	0.0000	0.0000
2.00	2.0175	2.0175	2.0175	2.0181	2.0181	2.2225	2.2453	2.2453	2.2255	2.2370	2.2370

Table 3
Result of HAM and BVP4c Matlab solver for $f'(\eta)$, $\theta(\eta)$ and $\phi(\eta)$ when $\lambda = 0.1$, $\beta_2 = 0.1$, $A = 0.1$, $S = 0.1$, $\Pr = 0.8$, $Sc = 0.9$, $K_s = 1$, $K = 0.4$.

η	$f'(\eta)$				$\theta(\eta)$				$\phi(\eta)$			
	$\beta_1 = 0$		$\beta_1 = 0.1$		$\beta_1 = 0$		$\beta_1 = 0.1$		$\beta_1 = 0$		$\beta_1 = 0.1$	
	HAM	BVP4c	HAM	BVP4c	HAM	BVP4c	HAM	BVP4c	HAM	BVP4c	HAM	BVP4c
0.0	1.000	1.000	1.000	1.000	1.000	1.000	1.000	1.000	1.000	1.000	1.000	1.000
0.5	0.5778	0.5750	0.6975	0.6909	0.5778	0.5750	0.5794	0.5750	0.5070	0.5027	0.5074	0.5074
1	0.5164	0.5175	0.6384	0.6310	0.5164	0.5175	0.5183	0.5117	0.7223	0.7220	0.7243	0.7242
1.5	0.4612	0.4651	0.5364	0.5343	0.4612	0.4651	0.4634	0.4651	0.7715	0.7710	0.7760	0.7760
2	0.4119	0.4131	0.4532	0.4503	0.4119	0.4131	0.4142	0.4131	0.8663	0.8640	0.8673	0.8670
2.5	0.3676	0.3669	0.4176	0.4131	0.3676	0.3669	0.3702	0.3790	0.9167	0.9161	0.9187	0.9185
3	0.2928	0.2936	0.3567	0.3553	0.2928	0.2936	0.3307	0.3332	0.9507	0.9500	0.9525	0.9525
3.5	0.2613	0.2642	0.3308	0.3332	0.2613	0.2642	0.2954	0.2936	0.9702	0.9692	0.9742	0.9740
4	0.2332	0.2339	0.2865	0.2846	0.2332	0.2339	0.2689	0.2642	0.9825	0.9803	0.9862	0.9862
4.5	0.2081	0.2079	0.2508	0.2532	0.2081	0.2079	0.2357	0.2339	0.9902	0.9892	0.9977	0.9976
5	0.1658	0.1641	0.2220	0.2262	0.1658	0.1641	0.1503	0.1504	0.9936	0.9920	0.9988	0.9987
5.5	0.1322	0.1319	0.1987	0.1996	0.1322	0.1319	0.1201	0.1205	0.9965	0.9950	0.9968	0.9968
6	0.1050	0.1050	0.1720	0.1720	0.1055	0.1055	0.1074	0.1074	0.9976	0.9960	0.9980	0.9980

series solution is shown in Table 1. Table 2 shows the comparison of $f''(0)$ with the previous results when $\lambda = 0$. Table 3 presents comparison between the HAM and BVP4c Matlab solver. This table reflects that both the results are in good agreement.

Main findings

We analyzed the stagnation point flow of an Oldroyd-B fluid under the influence of homogeneous/heterogeneous reaction. The main results are given below.

- The velocity and temperature have opposite behavior for larger values of Deborah number in terms of relaxation time.
- Similar trend is seen for the velocity and concentration distribution for higher values of Deborah number (through retardation time) while temperature gradient is opposite.
- Behavior of λ for the velocity and temperature profiles are opposite.
- Larger values of stratified variable corresponds to reduction in temperature and velocity profiles.
- Concentration have opposite trend via homogeneous and heterogeneous variables.

References

[1] Sajid M, Abbas Z, Javed T, Ali N. Boundary layer flow of an Oldroyd-B fluid in the region of stagnation point over a stretching sheet. Can J Phys 2010;88:635–40.
[2] Abbasbandy S, Hayat T, Alsaedi A, Rashidi MM. Numerical and analytical solutions for Falkner-Skan flow of MHD Oldroyd-B fluid. Int J Numer Methods Heat Fluid Flow 2014;24:390–401.
[3] Hayat T, Hussain T, Shehzad SA, Alsaedi A. Flow of Oldroyd-B fluid with nanoparticles and thermal radiation. Appl Math Mech 2015;36:69–80.
[4] Hayat T, Muhammad T, Shehzad SA, Alsaedi A. Temperature and concentration stratification effects in mixed convection flow of an Oldroyd-B fluid with thermal radiation and chemical reaction. Plos One 2015;10:e0127646.
[5] Ramzan M, Farooq M, Alhothuali MS, Malaikah HM, Cui W, Hayat T. Three dimensional flow of an Oldroyd-B fluid with Newtonian heating. Int J Numer Methods Heat Fluid Flow 2015;25:68–85.
[6] Mustafa M, Ahmad R, Hayat T, Alsaedi A. Rotating flow of viscoelastic fluid with nonlinear thermal radiation: a numerical study. Neural Comput Appl 2016:1–7.
[7] Hayat T, Qayyum S, Alsaedi A, Waqas M. Simultaneous influences of mixed convection and nonlinear thermal radiation in stagnation point flow of Oldroyd-B fluid towards an unsteady convectively heated stretched surface. J Mol Liq 2016;224:811–7.
[8] Hayat T, Muhammad T, Shehzad SA, Alsaedi Ahmed. An analytical solution for magnetohydrodynamic Oldroyd-B nanofluid flow induced by a stretching sheet with heat generation/absorption. Int J Therm Sci 2017;111:274–88.
[9] Hiemenz K. Die Grenzschicht an einem in den gleichfor murgen Flussigkeitsstrom eingentocuchten graden kreiszylinder. Dinglers Polytech J 1911;326:321–4.
[10] Turkyilmazoglu M, Pop I. Exact analytical solutions for the flow and heat transfer near the stagnation point on a stretching/shrinking sheet in a Jeffrey fluid. Int J Heat Mass Transf 2013;57:82–8.
[11] Mukhopadhyay S. Effects of partial slip on chemically reactive solute distribution in MHD boundary layer stagnation point flow past a stretching permeable sheet. Int J Chem Reactor Eng 2015;13:29–36.
[12] Hayat T, Farooq M, Alsaedi A. Thermally stratified stagnation point flow of Casson fluid with slip conditions. Int J Numer Methods Heat Fluid Flow 2015;25:724–48.
[13] Rashidi MM, Ali M, Freidoonimehr N, Rostami B, Hossain MA. Mixed convective heat transfer for MHD viscoelastic fluid flow over a porous wedge with thermal radiation. Adv Mech Eng 2014;6:735939.
[14] Shehzad SA, Hayat T, Alsaedi A, Ahmad B. Effects of thermophoresis and thermal radiation in mixed convection three-dimensional flow of Jeffrey fluid. Appl Math Mech 2015;36:655–68.
[15] Sui J, Zheng L, Zhang X, Chen G. Mixed convection heat transfer in power law fluids over a moving conveyor along an inclined plate. Int J Heat Mass Transfer 2015;85:1023–33.
[16] Ellahi R, Riaz A, Abbasbandy S, Hayat T, Vafai K. A study on the mixed convection boundary layer flow and heat transfer over a vertical slender cylinder. Therm Sci 2014;18:1247–58.
[17] Nawaz M, Zeeshan A, Ellahi R, Abbasbandy S, Rashidi S. Joules and Newtonian heating effects on stagnation point flow over a stretching surface by means of genetic algorithm and Nelder–Mead method. Int J Numerl Methods Heat Fluid Flow 2015;25:665–84.
[18] Ellahi R, Hassan M, Zeeshan A, Khan AA. The shape effects of nanoparticles suspended in HFE-7100 over wedge with entropy generation and mixed convection. Appl Nanosci 2016;6:641–51.
[19] Ellahi R, Hassan M, Zeeshan A. Aggregation effects on water base Al_2O_3 nanofluid over permeable wedge in mixed convection. AsiaPacific J Chem Eng 2016;11:179–86.
[20] Mamourian M, Shirvan KM, Ellahi R, Rahimi AB. Optimization of mixed convection heat transfer with entropy generation in a wavy surface square lid-driven cavity by means of Taguchi approach. Int J Heat Mass Transf 2016;102:544–54.
[21] Chaudhary MA, Merkin JH. A simple isothermal model for homogeneous-heterogeneous reactions in boundary-layer flow, I Equal diffusivities. Fluid Dyn Res 1995;16:311–33.
[22] Bhattacharyya K, Uddin MS, Layek GC, Ali W. Diffusion of chemically reactive species in boundary layer flow over a porous plate in porous medium. Chem Eng Commun 2013;200:1701–10.
[23] Hayat T, Hussain Z, Farooq M, Alsaedi A. Effects of homogeneous and heterogeneous reactions and melting heat in the viscoelastic fluid flow. J Mol Liq 2016;215:749–55.
[24] Hayat T, Farooq M, Alsaedi A. Homogeneous-heterogeneous reactions in the stagnation point flow of carbon nanotubes with Newtonian heating. AIP Adv 2015;5:027130.
[25] Hayat T, Hussain Z, Alsaedi A, Ahmad B. Heterogeneous-homogeneous reactions and melting heat transfer effects in flow with carbon nanotubes. J Mol Liq 2016;220:200–7.
[26] Imtiaz M, Hayat T, Alsaedi Ahmed. MHD convective flow of Jeffrey fluid due to a curved stretching surface with homogeneous-heterogeneous reactions. PloS one 2016;11:e0161641.
[27] Hayat T, Khan MI, Farooq M, Yasmeen T, Alsaedi A. Stagnation point flow with Cattaneo–Christov heat flux and homogeneous-heterogeneous reactions. J Mol Liq 2016;220:49–55.
[28] Farooq M, Alsaedi A, Hayat T. Note on characteristics of homogeneous-heterogeneous reaction in flow of Jeffrey fluid. Appl Math Mech 2015;36:1319–28.
[29] Hayat T, Hussain Z, Farooq M, Alsaedi A. Homogeneous and heterogeneous reactions effects in flow with Joule heating and viscous dissipation. J Mech 2016:1–10.
[30] Hayat T, Hussain Z, Farooq M, Alsaedi A, Obaid M. Thermally stratified stagnation point flow of an Oldroyd-B fluid. Int J Nonlinear Sci Numer Simul 2014;15:77–86.
[31] Hayat T, Hussain Z, Alsaedi A, Mustafa M. Nanofluid flow through a porous space with convective conditions and heterogeneous–homogeneous reactions. J Taiwan Inst Chem Eng 2016.
[32] Zheng L, Wang L, Zhang X. Analytic solutions of unsteady boundary flow and heat transfer on a permeable stretching sheet with non-uniform heat source/sink. Commun Nonlinear Sci Numer Simul 2011;16:731–40.
[33] Liao SJ. Homotopy analysis method in non-linear differential equations. Heidelberg: Springer and higher education press; 2012.
[34] Shehzad A, Ali R. MHD flow of a non-Newtonian Power law fluid over a vertical stretching sheet with the convective boundary condition. Walailak J Sci Tech 2012;10:43–56.
[35] Khan M, Ali R, Shahzad A. MHD Falkner-Skan flow with mixed convection and convective boundary conditions. Walailak J Sci Tech 2013;10:517–29.
[36] Aziz T, Mahomed FM, Shahzad A, Ali R. Travelling wave solutions for the unsteady flow of a third grade fluid induced due to impulsive motion of flat porous plate embedded in a porous medium. J Mech 2014;30:527–35.
[37] Farooq U, Zhao YL, Hayat T, Alsaedi A, Liao SJ. Application of the HAM-based Mathematica package BVPh 2.0 on MHD FalknerSkan flow of nano-fluid. Comput Fluids 2015;111:69–75.
[38] Ahmed J, Shahzad A, Khan M, Ali R. A note on convective heat transfer of an MHD Jeffrey fluid over a stretching sheet. AIP Adv 2015;5. 117–117.
[39] Hayat T, Hussain Z, Alsaedi A, Asghar S. Carbon nanotubes effects in the stagnation point flow towards a nonlinear stretching sheet with variable thickness. Adv Powder Technol 2016;27:1677–88.
[40] Hayat T, Hussain Z, Muhammad T, Alsaedi Ahmed. Effects of homogeneous and heterogeneous reactions in flow of nanofluids over a nonlinear stretching surface with variable surface thickness. J Mol Liq 2016;221:1121–7.
[41] Shahzad A, Ali R, Hussain M, Kamran M. Unsteady axisymmetric flow and heat transfer over time-dependent radially stretching sheet. Alexandria Eng J 2016.
[42] Hayat T, Hussain Z, Farooq M, Alsaedi Ahmed. MHD flow of Powell-Eyring fluid by a stretching cylinder with newtonian heating. Therm Sci 2016. 162–162.
[43] Hayat T, Hussain Z, Alsaedi A, Farooq M. Magnetohydrodynamic flow by a stretching cylinder with Newtonian heating and homogeneous-heterogeneous reactions. PloS one 2016;11:e0156955.
[44] Hayat T, Bashir G, Waqas M, Alsaedi A. MHD flow of Jeffrey liquid due to a nonlinear radially stretched sheet in presence of Newtonian heating. Results Phys 2016.
[45] Mahapatra TR, Gupta AS. Heat transfer in stagnation-point flow of a micropolar fluid towards a stretching sheet. Heat Mass Transf 2002;38: 517–21.
[46] Nazar R, Amin N, Filip D, Pop I. Stagnation point flow of a micropolar fluid towards a stretching sheet. Int J Non-Linear Mech 2004;39:1227–35.